Separation Science and Technology
Publication details, including instructions for authors and subscription information:
http://www.informaworld.com/smpp/title~content=t713708471

Experimental design approach for the optimization of the separation of enantiomers in preparative liquid chromatography

Shih-Ming Lai[a]; Zi-Chin Lin[a]
[a] Department of Chemical Engineering, National Yunlin University of Science and Technology, Yunlin, Taiwan, ROC

Online publication date: 23 April 2002

To cite this Article Lai, Shih-Ming and Lin, Zi-Chin(2002) 'Experimental design approach for the optimization of the separation of enantiomers in preparative liquid chromatography', Separation Science and Technology, 37: 4, 847 — 875
To link to this Article: DOI: 10.1081/SS-120002220
URL: http://dx.doi.org/10.1081/SS-120002220

SEPERATION SCIENCE AND TECHNOLOGY, 37(4), 847–875 (2002)

EXPERIMENTAL DESIGN APPROACH FOR THE OPTIMIZATION OF THE SEPARATION OF ENANTIOMERS IN PREPARATIVE LIQUID CHROMATOGRAPHY

Shih-Ming Lai* and Zi-Chin Lin

Department of Chemical Engineering, National Yunlin University of Science and Technology, 123 Sec. 3, University Road, Touliu, Yunlin, Taiwan, ROC

ABSTRACT

The preparative separation of enantiomers of 1-1′-bi-2-naphthol on Pirkle covalent D-phenylglycine columns using hexane/isopropanol as the mobile phase was performed under a range of experimental conditions of flow rate, sample size, and mobile-phase composition. The system performance was evaluated based on the production rate with or without solvent consumption. Factorial design experiments using a spherical central composite design, with three variables (at five levels each) and the related response functions, were conducted to study the effect of the individual variables on the response functions. The regression models of the response functions were then established by second-order polynomials consisting of linear, quadratic, and interaction terms. The hybrid objective function (tradeoff between the

*Corresponding author. Fax: (886) 5-531-2071; E-mail: laism@pine.yuntech.edu.tw

production rate and solvent consumption) together with some constraints (e.g., constraints on purity, recovery yield, amount injected, and flow rate) were considered. The optimum level of these variables for obtaining maximum magnitude of the hybrid objective function were found and further verified experimentally.

Key Words: Enantiomeric separation; Preparative scale; System performance; Optimization; Experimental design and analysis

INTRODUCTION

The separation of enantiomers has been an important issue in the fields of pharmacy, agrochemicals, food, and petrochemicals. Currently, there is a considerable demand for the preparative-scale techniques for the separation of enantiomers. High performance liquid chromatography (HPLC) using chiral stationary phases (CSPs) is by far the most widely used technique employed today for the effective and massive separations of enantiomers. However, the separation factors obtained for chiral separations are frequently very low, being the order of 1.1–1.5, which makes enantio-separation difficult on a preparative scale (1,2).

Optimization of the production rate is an important practical problem. Production rate is affected mainly by the following operating variables: column length, particle size, flow rate, sample size, and mobile-phase composition. Generally, separations are optimized by a trial and error method—a procedure that may be tedious and prolonged as it involves many experiments. Theoretical modeling leads to a better understanding of the phenomena and may be used to predict the band profiles and to optimize the system performance. Nevertheless, the reliability of simulation has to be built on the accurate adsorption isotherm equation and on the value of the parameters (3–5). However, determination of the coefficients of competitive adsorption isotherms between enantiomers requires a lot of experimental work, which is very time-consuming and costly in terms of the materials required. In addition, very often the simulated band profiles cannot predict the tailing phenomenon of the earlier eluted isomer effectively, which leads to inaccuracy in predicting the system performance by the theoretical model (6). Another alternative and straightforward way is by using the experimental design together with multiple regressions, which simplifies the optimization procedure effectively. Response surface resulting from the fitted regression model can be used to find the relationship of a set of controlled experimental factors and observed responses and to predict finally the optimum operating conditions (7).

The preparative separation of enantiomers of 1-1′-bi-2-naphthol on Pirkle covalent D-phenylglycine (3,5-dinitrobenzoyl derivative of phenylglycine covalently bonded to aminopropyl silica gel) columns using hexane/isopropanol as the mobile phase was considered as a model system in this study. Optically pure enantiomers of 1-1′-bi-2-naphthol can be used as the chiral precursor of various optically active catalysts used in enantioselective syntheses (8,9). Since the column design parameters, e.g., column length and particle size, were fixed in our system, the main operating variables affecting the production rate thus included flow rate, sample size, and mobile-phase composition. Little attention has been given to the proper selection of mobile-phase composition, which is known to have great effects on the retention times, the separation factor, the solubility of racemic mixtures, the maximum flow rate allowed, and the system performance (6).

In the present investigation, factorial design experiments using a spherical central composite design (10), with the above three operating variables and the response functions (production rate with or without solvent consumption was considered), were conducted to study the effect of the individual variables on the response functions. The regression models were then established by second-order polynomials consisting of linear, quadratic, and interaction terms. In addition, the hybrid objective function (tradeoff between the production rate and solvent consumption) together with some constraints (e.g., constraints on purity, recovery yield, amount injected, and flow rate) were considered. Finally, the optimum operating conditions for maximizing the hybrid objective function were found and further verified experimentally.

THEORY

System Performance Indices

Figure 1 shows the chromatogram of an overloaded injection. The collection period for a component i is determined by the purity requirement, e.g., 98%.

The recovery yield, Y_i, is defined as the ratio of the amount of a component i collected in the purified fraction to the total amount of this component injected with the sample:

$$Y_i = \frac{\text{amount collected}}{\text{amount injected}} = \frac{\int_{t_{ci,1}}^{t_{ci,2}} Q_f C_i \mathrm{d}t}{V_{in} \cdot C_i^0}; \quad i = R, S \tag{1}$$

where Q_f is the solvent flow rate, V_{in} is the sample volume, C_i^0 is the inlet concentration of component i (C_i^0 equals a half of the inlet concentration of the

MARCEL DEKKER, INC.
270 Madison Avenue, New York, New York 10016

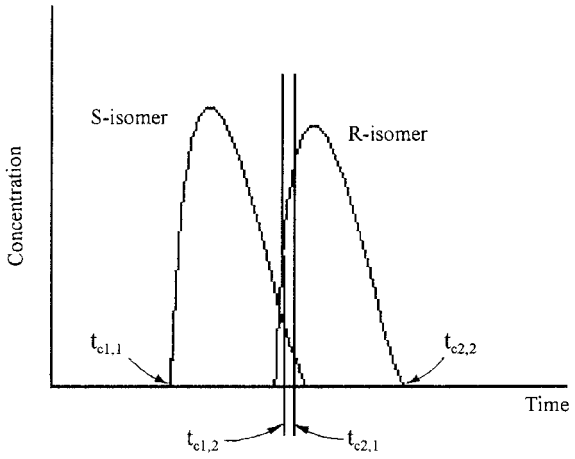

Figure 1. Schematic diagram of overloaded band profiles of a racemic mixture.

racemic mixture, C^0), and $t_{ci,1}$ and $t_{ci,2}$, as shown in Fig. 1, are the beginning and end times of the collection of component i, respectively.

The production rate, Pr_i, is the amount of a component i collected in the fraction at the specified purity per unit time:

$$\mathrm{Pr}_i = \frac{\text{amount collected}}{\text{cycle time}} = \frac{V_{\text{in}} \cdot C_i^0 \cdot Y_i}{\Delta t_{\text{c}}};\ i = R, S \tag{2}$$

where Δt_{c} is the cycle time that separates two consecutive injections and is defined as the time difference between the time when the first component concentration exceeds a certain threshold, e.g., 1×10^{-6}, and the time when the second component concentration decreases below this threshold value.

The specific production, SP_i, is defined as the amount of purified product obtained by using a unit amount of solvent:

$$\mathrm{SP}_i = \frac{\mathrm{Pr}_i}{Q_{\text{f}}} = \frac{V_{\text{in}} \cdot C_i^0 \cdot Y_i}{\Delta t_{\text{c}} \cdot Q_{\text{f}}};\quad i = R, S \tag{3}$$

which is the reciprocal of the solvent consumption.

Experimental Design

The three independent variables for the separation of enantiomers were: flow rate ($X_1 = \mathrm{Q_f}$, mL/min), sample concentration ($X_2 = \mathrm{C}^0$, mg/mL) and mobile-phase composition (X_3, hexane%). A spherical central composite design

Table 1. Experimental Design Matrix in Coded and Actual Level of Variables

	Flow Rate		Sample Concentration		Mobile-Phase Composition	
Run No.	Coded Level x_1	Actual Level X_1 (mL/min)	Coded Level x_2	Actual Level X_2 (mg/mL)	Coded Level x_3	Actual Level X_3 (hexane%)
1	−1	6	−1	2.0	−1	75
2	1	12	−1	2.0	−1	75
3	−1	6	1	5.0	−1	75
4	1	12	1	5.0	−1	75
5	−1	6	−1	2.0	1	85
6	1	12	−1	2.0	1	85
7	−1	6	1	5.0	1	85
8	1	12	1	5.0	1	85
9	0	9	0	3.5	0	80
10	0	9	0	3.5	0	80
11	0	9	0	3.5	0	80
12	1.6	13.8	0	3.5	0	80
13	−1.6	4.2	0	3.5	0	80
14	0	9	1.6	5.9	0	80
15	0	9	−1.6	1.1	0	80
16	0	9	0	3.5	1.6	88
17	0	9	0	3.5	−1.6	72

MARCEL DEKKER, INC.
270 Madison Avenue, New York, New York 10016

(10) was used and the experimental design matrix consisting of a set of 17 experiments in the actual (X) and coded (x) levels of variables is shown in Table 1. The method employed was a three-variable (five levels of each variable), second-order orthogonal design with three replications at the center points $(0, 0, 0)$, in coded levels of variables $(-1.6, -1, 0, 1, 1.6)$.

The system performances, including production rate and specific production, were calculated by the two measurable quantities, i.e., amount collected and cycle time. They were selected as the response functions and were approximated by a second-degree polynomial with linear, quadratic, and interaction effects (in coded level of variables) as:

$$y_k = b_0 + \sum_{j=1}^{n} b_i x_i + \sum_{i=1}^{n} \sum_{j=1}^{n} b_{ij} x_i x_j (i \leq j) + \epsilon \tag{4}$$

The number of variables is denoted by n, and i, j, and k are integers. The coefficients of the polynomials are represented by b_0, b_i, and b_{ij}, which can be solved by the method of least squares (7), and ϵ is the random number. The response surface graphs can be obtained from the regression equations in actual level of variables, keeping the response function on the Z axis with X and Y axes representing the two independent variables while keeping the other one variable constant.

Optimization

A hybrid objective function, Pr_i^*, in which the importance of both the production rate and the specific production (solvent consumption) are considered, is defined as (11):

$$\frac{1}{\mathrm{Pr}_i^*} = \frac{(1-w)}{\mathrm{Pr}_i} + \frac{w}{\mathrm{SP}_i} \tag{5}$$

where the weight factor w $(0 \leq w \leq 1)$ represents the significance of the production rate or solvent consumption. If $w = 0$, the production rate is considered regardless of the solvent consumption. If $w = 1$, the specific production is considered as the objective function. Intermediate values of w result in a tradeoff between production rate and solvent consumption.

In the optimization process, the solubility limit and maximum flow rate with respect to mobile-phase composition were used as the inequality constraints and the required purity and recovery yield were used as the equality constraints. Then the optimization problem can be expressed as follows:

$$\max_{X_1, X_2, X_3} \mathrm{Pr}_i^* \text{ with : purity} = 0.98, \quad Y_i = 0.95 \text{ or } 0.90 \tag{6}$$

where $X_1 \leq$ maximum flow rate, and $X_2 \leq$ solubility limit.

Marcel Dekker, Inc.
270 Madison Avenue, New York, New York 10016

Optimization was done by using software—constr [SQP algorithm (12)] available in MATLAB optimization toolbox, wherein the levels of the three variables were determined to obtain the maximum Pr_i^*.

EXPERIMENTAL

Materials

The separation of 1-1′-bi-2-naphthol enantiomers using Pirkle covalent D-phenylglycine (3,5-dinitrobenzoyl derivative of phenylglycine covalently bonded to aminopropyl silica gel) as CSP and mobile-phase composition ranging from 70/30 to 90/10 (vol/vol) hexane/isopropanol (IPA) as eluent was studied.

Stationary Phase

The CSP columns purchased from Regis (Morton Grove, IL, USA) were used in this study. The column dimensions were of 25 cm length × 0.46 cm i.d. (the analytical column) and 25 cm length × 1.0 cm i.d. (the preparative column). The particle diameters were 5 μm for both columns.

Chemicals and Solvents

(*R*)-(+)-1-1′-bi-2-naphthol (*R*-isomer, 99% pure, formula weight 286.33), (*S*)-(−)-1-1′-bi-2-naphthol (*S*-isomer, 99% pure, formula weight 286.33), and 1-1′-bi-2-naphthol (racemic mixture, 99% pure, formula weight 286.33) were purchased from Aldrich (Milwaukee, WI). The HPLC grade hexane and IPA were purchased from Tedia (Fairfield, OH).

Apparatus

An HPLC system includes a Jasco Model PU980 solvent metering pump, a Jasco Model UV970 UV detector (Tokyo, Japan), a Rheodyne Model 7125 six-way syringe loading valve fitted with a 20-μL or a 2-mL sample loop (Cotati, CA), and a Sunway Model 940-CO column oven (Taipei, Taiwan). The system was thermostatted at 30°C. The millivolt signal from the detector was converted to digital form with the aid of an analog-to-digital interface card (Scientific Information Service Corp., Taipei, Taiwan) interfaced with a microcomputer for data storage and processing. In addition, an ISCO Retriever 500 fraction collector (Lincoln, NE) was used to complement the HPLC system.

MARCEL DEKKER, INC.
270 Madison Avenue, New York, New York 10016

Measurement of Overloaded Band Profiles

There were two types of calibration curves used in transforming detector response into concentration. As the UV spectrum is the same for both enantiomers, only one calibration was necessary. The first type was derived from experimental absorbances measured for the standard solution of each compound studied. The wavelength was chosen as 347 nm by which the high concentration range was covered (till 3.0 mg/mL) and the detector response was nonlinear. Conversion of the detector response profiles into concentration profiles was accomplished by using a parabolic concentration vs. response calibration graph, which can be expressed by the following equation:

$$y = 1.5093 \times 10^{-6} x^2 + 0.00208x + 0.0176 \tag{7}$$

where x is the detector response (mV), and y the concentration (mg/mL).

The second type was determined by using standard analytical techniques. The fractions injected into the analytical column were small (20-μL) and dilute enough that their analysis could be carried out under linear conditions. The peak areas were calculated from the detector responses monitored at 254 nm. Then a linear calibration graph of concentration vs. peak area was determined by a least-squares fit, which can be expressed by the following equation:

$$y = 9.9237 \times 10^{-7} x \tag{8}$$

where x is the peak area (sec μV), and y the concentration (mg/mL).

To determine the individual concentrations of each of the antipodes in the mixed-band region of the elution profile, fractions of the band profiles were collected during the elution of high-concentration binary bands. The fractions were collected at 0.1–0.2 min intervals from the start and through the end of the mixed zone. Then aliquots of these fractions were injected subsequently under analytical conditions where complete separation of these samples occurred. The concentrations of each enantiomer at each collection time can be calculated by the linear calibration graph of concentration vs. peak area, and the individual experimental elution profiles are regenerated.

Measurement of Effect of Mobile-Phase Composition on Sample Concentration and Flow Rate

The increase in the sample concentration (X_2) is limited by its solubility limit. The mobile-phase composition (X_3) has a great effect on the solubility limit of the racemic mixture. The solubility limit at each of the mobile-phase compositions (hexane%, $X_3 = 70,\ 75,\ 80,\ 85,\ 90,\ 95$) was measured by the

MARCEL DEKKER, INC.
270 Madison Avenue, New York, New York 10016

following procedure. First, at each mobile-phase composition, the supersaturated solution of the racemic mixture was prepared and shaken in a water bath at 30°C for several hours. Then, the clear supernatant of the upper layer of each solution was collected and analyzed by liquid chromatography under analytical conditions. Finally, the concentration, i.e., the solubility limit of the racemic mixture at each mobile-phase concentration, was calculated by the linear calibration graph of concentration vs. peak area [Eq. (8)]. A linear calibration graph of solubility limit vs. mobile-phase concentration was then determined by a least-squares fit, which can be expressed by the following equation:

$$y = -0.4772x + 47.4307 \tag{9}$$

where x is the mobile-phase concentration (hexane%), and y the solubility limit (mg/mL).

The mobile-phase composition (X_3) also has a great effect on the maximum flow rate (X_1) allowed in this liquid chromatographic system. The maximum flow rate allowed at each of the mobile-phase compositions (hexane%, $X_3 = 60, 65, 70, 75, 80, 85, 90, 95$) was measured by setting the maximum inlet pressure allowed at 180 kg/cm^2. The results show that the maximum flow rate allowed increases linearly with increase in the level of hexane% in the mobile phase. The linear calibration graph of maximum flow rate vs. mobile-phase concentration was then least-square fitted by the following equation:

$$y = 0.3579x - 6.8138 \tag{10}$$

where x is the mobile-phase concentration (hexane%), and y the maximum flow rate (mL/min).

RESULTS AND DISCUSSION

For our model system, i.e., 1-1′-bi-2-naphthol separated on Pirkle covalent D-phenylglycine column using hexane/isopropanol as the mobile phase, the *S*-isomer species is less retained than the *R*-isomer species. The retention of each isomer and the separation factor increase with increasing hexane% in the mobile phase (6).

Since the 2-mL sample loop was used for all the preparative injections, the sample size is directly proportional to the sample concentration. The experimental results on the effect of the three variables (flow rate, sample concentration, and mobile-phase composition) on the selected response functions (purity for each isomer was set at 0.98) are shown in Table 2. Each experiment was at least duplicated under identical conditions. The relative standard deviation

was mostly within 1%, therefore, the data in Table 2 were taken from their average values.

Regression Analysis

The condensed analysis of variances (ANOVA) table (in coded level of variables), including the coefficients of the regression model [Eq. (4)], *t*-statistics, and significance probabilities, is shown in Table 3 for the above response functions. The high correlation coefficient for each regression model ($R^2 \geq 0.98$, except $R^2 = 0.94$ for the production rate of the *R*-isomer) indicates the suitability of the second-order polynomial to predict each response function.

Effect of Operating Variables

The response surfaces, obtained from the regression equations in actual level of variables within the experimental range, are shown in Figs. 2–8 to aid in visualizing the effect of the three operating variables. Here, the *Z* axis represents the response function and *X* and *Y* axes represent the two independent variables while keeping the third variable constant at its center point.

The effect of operating variables on the cycle time is shown in Fig. 2. The cycle time increases only slightly with increasing sample concentration, but decreases significantly with increasing flow rate and decreasing hexane% in the mobile phase (Table 3 and Fig. 2). An asymptotic value of the cycle time (about 1 min) is reached at a high level of flow rate and low level of hexane% in the mobile phase (Fig. 2b).

The effect of operating variables on the amount collected for the *S*- and *R*-isomers is shown in Figs. 3 and 4, respectively. From our previous study (6), for the less retained *S*-isomer, the amount collected is less affected by the overlap with the opposite isomer leading to a high recovery yield ($Y_S \geq 0.9$) for all 17 cases (Table 2). However, for the more retained *R*-isomer, the amount collected is much affected by the overlap with the opposite isomer leading to a low recovery yield ($Y_R \leq 0.5$) for some cases of low hexane% in the mobile phase (Table 2). Of the individual variables for the *S*-isomer, the sample concentration has the maximum positive linear effect followed by the less significant positive effect of hexane% in the mobile phase, but flow rate has nearly no effect (Table 3). Due to the less influence of band overlapping for the *S*-isomer, low levels of hexane% in the mobile phase can be used to increase the concentration of the sample injection (higher solubility limit) and then the collection amount of the *S*-isomer (Fig. 3c). Of the individual variables for the *R*-isomer, hexane% in the mobile phase has the maximum positive effect followed by the positive effect of the sample

MARCEL DEKKER, INC.
270 Madison Avenue, New York, New York 10016

Table 2. Experimental Results for the Response Functions

		Amount Collected[a] (mg)		Recovery Yield		Production Rate (mg/min)		Specific Production (mg/mL)	
Run No.	Cycle Time (min)	*S*-Isomer	*R*-Isomer	*S*-Isomer	*R*-Isomer	*S*-Isomer	*R*-Isomer	*S*-Isomer	*R*-Isomer
1	2.25	1.94	0.98	0.97	0.49	0.86	0.44	0.14	0.07
2	1.14	1.83	0.85	0.92	0.42	1.61	0.75	0.13	0.06
3	2.35	4.62	1.91	0.92	0.38	1.97	0.81	0.33	0.14
4	1.20	4.54	1.07	0.91	0.21	3.80	0.90	0.32	0.07
5	2.89	1.98	1.82	0.99	0.91	0.69	0.63	0.11	0.10
6	1.68	1.98	1.89	0.99	0.95	1.18	1.13	0.10	0.09
7	3.18	4.94	4.82	0.99	0.96	1.55	1.51	0.26	0.25
8	1.83	4.85	4.97	0.97	0.99	2.65	2.71	0.22	0.23
9	1.48	3.35	2.70	0.96	0.77	2.26	1.82	0.25	0.20
10	1.65	3.36	2.46	0.96	0.70	2.04	1.50	0.23	0.17
11	1.72	3.39	2.81	0.97	0.80	1.97	1.63	0.22	0.18
12	1.23	3.42	3.19	0.98	0.91	2.78	2.60	0.20	0.19
13	3.29	3.39	2.87	0.97	0.82	1.03	0.87	0.25	0.21
14	1.87	5.52	2.94	0.94	0.50	2.95	1.57	0.33	0.17
15	1.54	1.09	0.90	0.99	0.82	0.70	0.59	0.08	0.07
16	2.25	3.45	3.39	0.99	0.97	1.53	1.50	0.17	0.17
17	1.41	3.11	0.51	0.89	0.15	2.22	0.37	0.25	0.04

[a] Purity was set at 98% for each isomer.

MARCEL DEKKER, INC. 270 Madison Avenue, New York, New York 10016

Table 3. Regression Coefficients (in Coded Level), *t*-Statistics, and Probabilities Significance for Study Cases

	Cycle Time		Amount Collected			
			S-Isomer		*R*-Isomer	
Source of Variation	Regression Coefficient	*t*-Value	Regression Coefficient	*t*-Value	Regression Coefficient	*t*-Value
Constant	1.603	—	3.367	—	2.648	—
x_1	−0.619	−22.289***	−0.018	-1.729^{NS}	−0.017	-0.209^{NS}
x_2	0.086	3.084**	1.396	135.987***	0.800	9.918***
x_3	0.306	11.011***	0.104	10.098***	1.013	12.552***
x_1^2	0.272	8.542***	0.017	1.471^{NS}	0.160	1.726^{NS}
x_2^2	0.057	1.802*	−0.023	−0.909*	−0.273	−2.952**
x_3^2	0.105	3.300**	−0.030	−2.538**	−0.262	−2.826**
x_1x_2	−0.022	-0.630^{NS}	−0.006	-0.466^{NS}	−0.079	-0.765^{NS}
x_1x_3	−0.036	-1.004^{NS}	0.012	0.943^{NS}	0.150	1.450^{NS}
x_2x_3	0.036	1.018^{NS}	0.055	4.194***	0.615	5.955***
R^2	0.990		0.999		0.978	

MARCEL DEKKER, INC.
270 Madison Avenue, New York, New York 10016

	Production Rate				Specific Production			
	S-Isomer		*R*-Isomer		*S*-Isomer		*R*-Isomer	
	Regression Coefficient	*t*-Value	Regression Coefficient	*t*-Value	Regression Coefficient	*t*-Value	Regression Coefficient	*t*-Value
Constant	2.099	—	1.661	—	0.234	—	0.184	—
x_1	0.531	16.655***	0.370	5.362***	−0.011	−3.586***	−0.011	−2.703**
x_2	0.703	22.035***	0.349	5.059***	0.079	25.468***	0.041	10.272***
x_3	−0.250	−7.821***	0.374	5.412***	−0.027	−8.693***	0.041	10.332***
x_1^2	−0.084	−2.293*	0.015	0.184^{NS}	−0.005	-1.447^{NS}	0.004	0.953^{NS}
x_2^2	−0.116	−3.166**	−0.243	−3.067**	−0.013	−3.746***	−0.026	−5.817***
x_3^2	−0.097	−2.645**	−0.299	−3.772***	−0.011	−3.148***	−0.033	−7.189***
x_1x_2	0.211	5.174***	0.059	0.670^{NS}	−0.003	-0.733^{NS}	−0.008	-1.634^{NS}
x_1x_3	−0.125	−3.050**	0.162	1.836^{NS}	−0.004	-1.070^{NS}	0.004	0.835^{NS}
x_2x_3	−0.120	−2.939**	0.243	2.745*	−0.013	−3.150***	0.026	5.053***
R^2	0.992		0.943		0.991		0.979	

NS: nonsignificant at $P \geq 0.1$; *: significant at $0.05 \leq P \leq 0.10$; **: significant at $0.01 \leq P \leq 0.05$; ***: significant at $P \leq 0.01$.

MARCEL DEKKER, INC.
270 Madison Avenue, New York, New York 10016

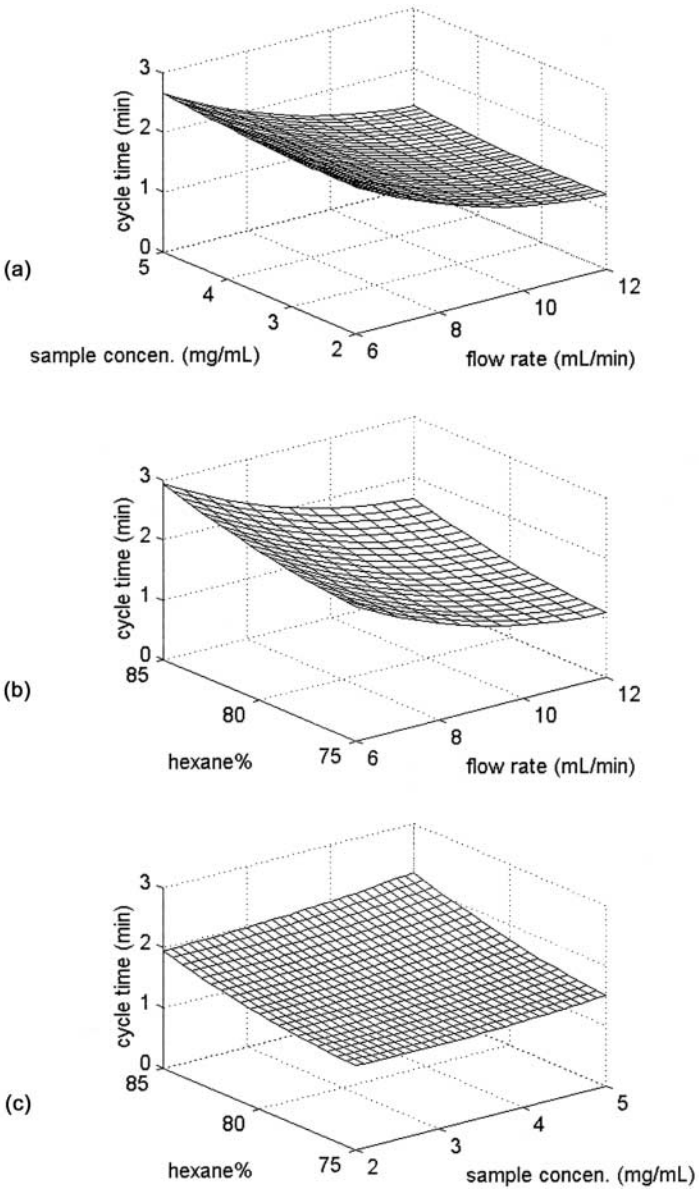

Figure 2. Response surface plot of the cycle time.

MARCEL DEKKER, INC.
270 Madison Avenue, New York, New York 10016

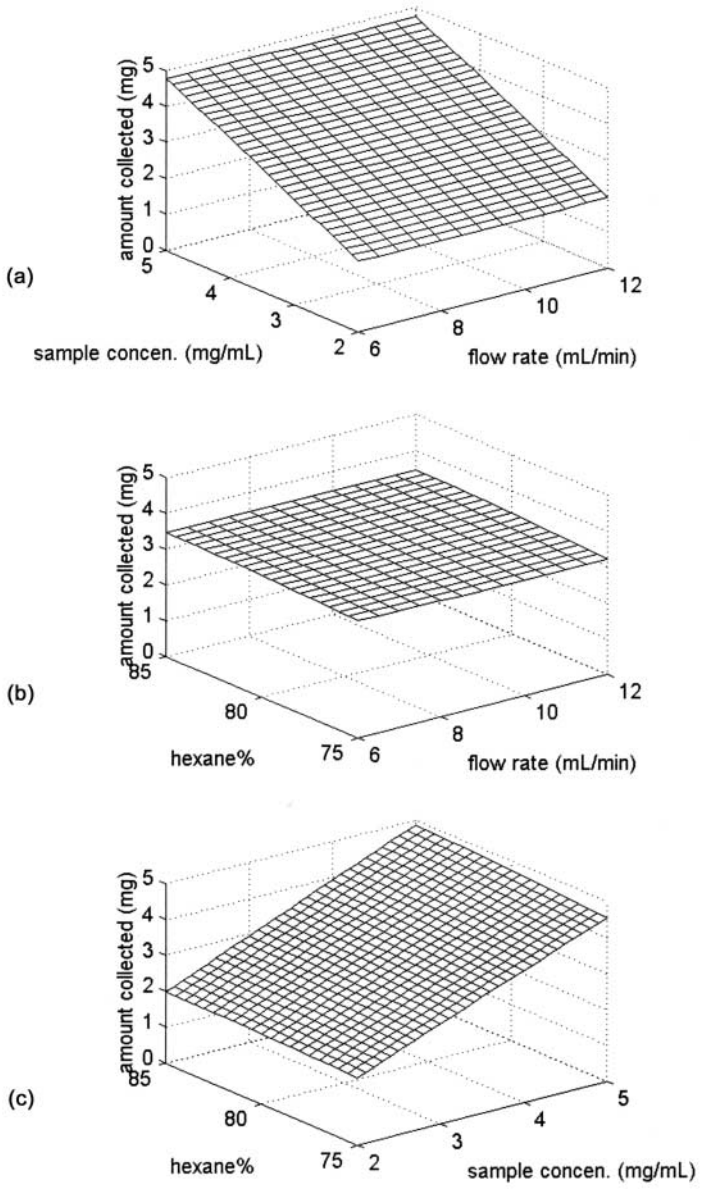

Figure 3. Response surface plot of the amount collected of the *S*-isomer.

MARCEL DEKKER, INC.
270 Madison Avenue, New York, New York 10016

concentration, and, similar to the *S*-isomer, the flow rate has nearly no effect (Table 3). Due to the high influence of band overlapping for the *R*-isomer, only high level of hexane% in the mobile phase is allowed to be used, and the concentration of sample injection and the collection amount of the *R*-isomer are therefore limited accordingly (Fig. 4c).

The production rate, defined by Eq. (2), was then calculated by the relative value of amount collected and cycle time (amount collected/cycle time). The effect of operating variables on the production rate for the *S*- and *R*-isomers is shown in Figs. 5 and 6, respectively. All the three operating variables are significant here. Of the individual variables, sample concentration and flow rate have the same positive effect for each isomer, but hexane% in the mobile phase has different effects for different isomers, i.e., negative effect for the *S*-isomer and positive effect for the *R*-isomer (Table 3). This is due to the overall effect of hexane% in the mobile phase on the concentration of sample injection (solubility limit) and the amount collected for different isomers (as explained above by the different effects of band overlapping). For the *S*-isomer, the production rate increases with increasing sample concentration, flow rate, and decreasing hexane% in the mobile phase (Fig. 5). However, for the *R*-isomer, the production rate increases with increasing sample concentration, flow rate, but increasing hexane% in the mobile phase (Fig. 6).

The specific production, defined by Eq. (3), was then calculated by the relative value of production rate and flow rate (production rate/flow rate). The effect of operating variables on the specific production for the *S*- and *R*-isomers is shown in Figs. 7 and 8, respectively. Again, all the three operating variables are significant here. The effect of sample concentration (positive effect) and hexane% in the mobile phase (negative effect for the *S*-isomer and positive effect for the *R*-isomer) on the specific production is the same as the effect on the production rate. However, due to the solvent consumption consideration, flow rate has a negative effect on the specific production for each isomer (Table 3). The specific production increases with increasing sample concentration and decreasing flow rate for each isomer, but decreases with increasing hexane% in the mobile phase for the *S*-isomer (Fig. 7) and increases with increasing hexane% in the mobile phase for the *R*-isomer (Fig. 8).

In summary, in order to optimize both the production rate and the specific production (solvent consumption), hexane% in the mobile phase can be low for the *S*-isomer ($<80\%$), but should be high for the *R*-isomer ($>85\%$). Sample concentration can be as high as possible under its solubility limit (determined by the hexane% in the mobile phase) for each isomer, however, the recovery yield, decreasing with increasing sample concentration, should be kept at a certain level ($Y_i > 0.90$ or 0.95). Finally, the maximum production rate can be reached at high flow-rate conditions, while the minimum solvent consumption must be operated at low flow-rate conditions. Thus, the operating flow-rate condition should be

MARCEL DEKKER, INC.
270 Madison Avenue, New York, New York 10016

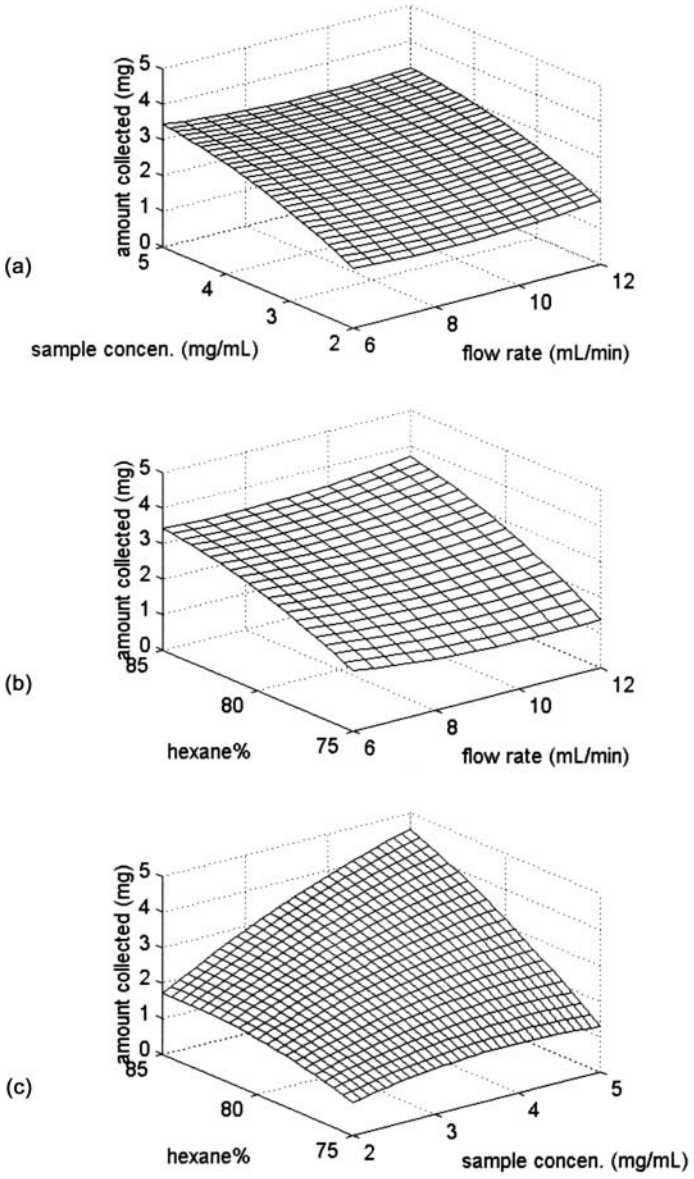

Figure 4. Response surface plot of the amount collected of the *R*-isomer.

MARCEL DEKKER, INC.
270 Madison Avenue, New York, New York 10016

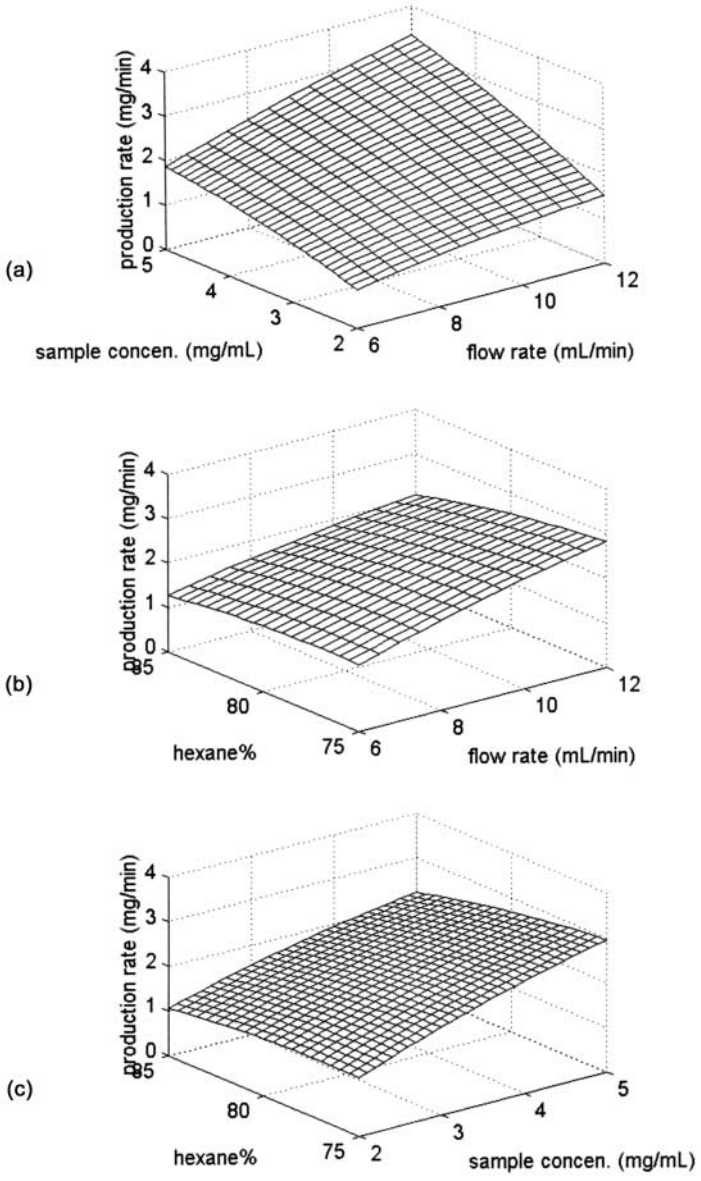

Figure 5. Response surface plot of the production rate of the *S*-isomer.

MARCEL DEKKER, INC.
270 Madison Avenue, New York, New York 10016

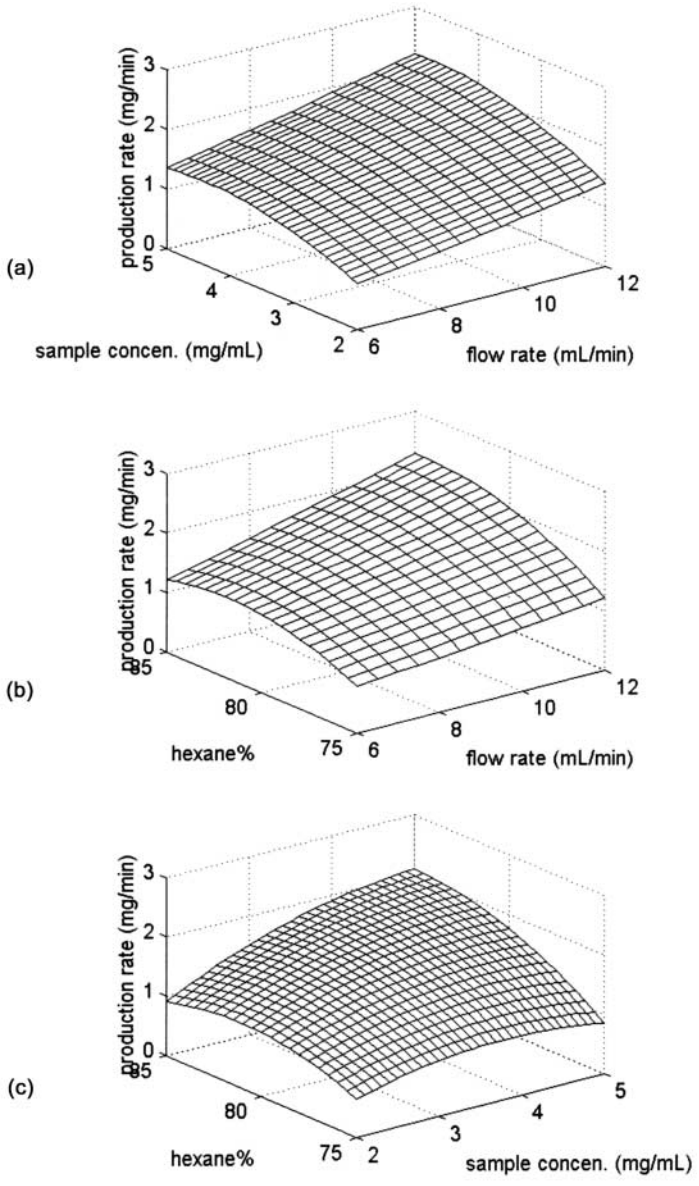

Figure 6. Response surface plot of the production rate of the *R*-isomer.

MARCEL DEKKER, INC.
270 Madison Avenue, New York, New York 10016

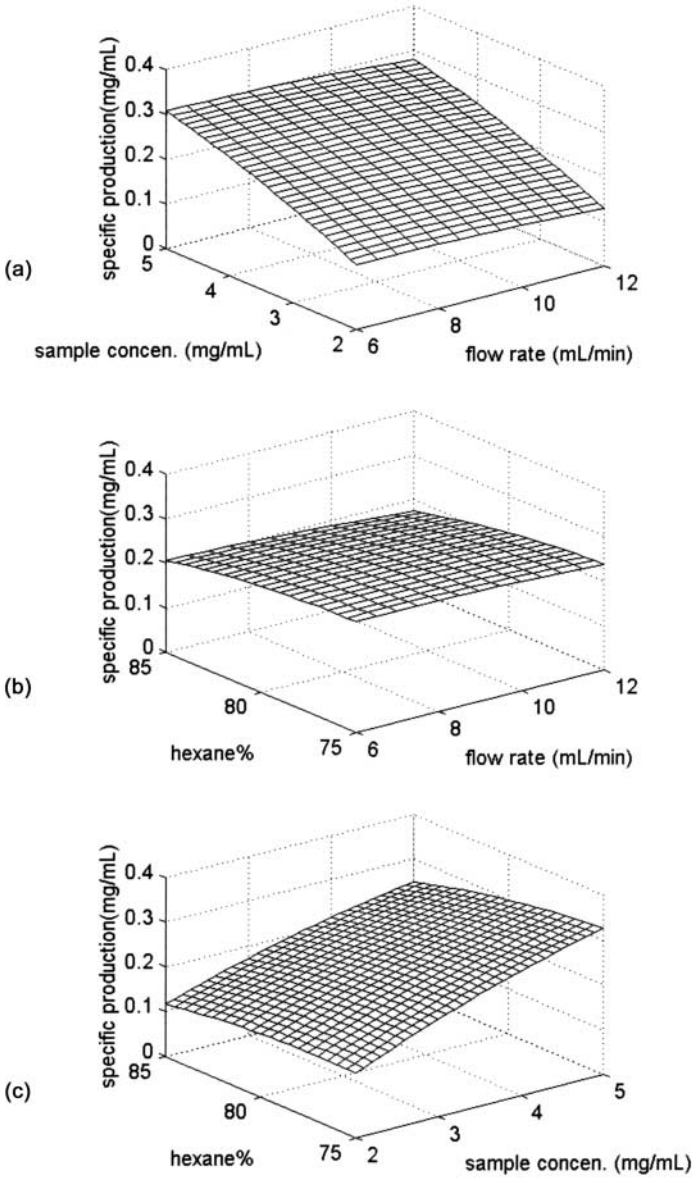

Figure 7. Response surface plot of the specific production of the *S*-isomer.

MARCEL DEKKER, INC.
270 Madison Avenue, New York, New York 10016

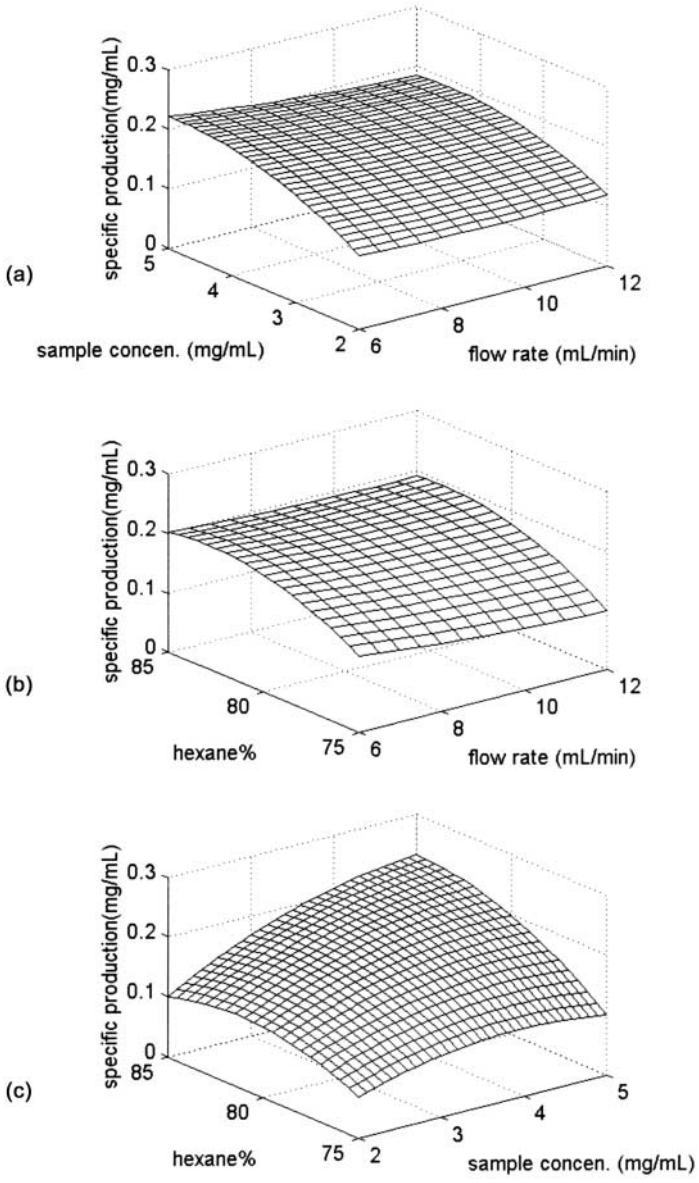

Figure 8. Response surface plot of the specific production of the *R*-isomer.

MARCEL DEKKER, INC.
270 Madison Avenue, New York, New York 10016

optimized on the basis of a compromise between the high production rate and the low solvent consumption.

Optimization and Experimental Verification of the Optimum Operating Conditions

As shown above, the optimum operating conditions for maximum production rate and for maximum specific production (minimum solvent consumption) are quite different. As a tradeoff between these two response functions, the hybrid objective function with a given weight, defined by Eq. (5), was used to consider the importance of the production rate and of the solvent consumption. Meanwhile, the optimum operating conditions should be selected depending on which isomer is desired.

The optimization problem, defined by Eq. (6), was solved using MATLAB optimization software—constr (constrained minimization or maximization). The regression models of the two measurable quantities, i.e., amount collected and cycle time, were used for the optimization. The optimization results in terms of the optimum operating conditions and system performance are shown in Tables 4 and 5 for the *S*-isomer and *R*-isomer, respectively. As expected, the production rate and the solvent consumption decreased with increasing the weight factor w, and it can be seen that the solvent consumption was reduced significantly without losing too much in the production rate at the level of w in between 0.05 and 0.10. It is also noted that when the weight factor w was larger than 0.05, the optimum operating conditions were all located within the experimental range, in which the reliability of the regression models can be guaranteed.

In summary, by defining the level of w in between 0.05 and 0.10, the following optimum operating parameters were found. For the *S*-isomer, if a recovery yield higher than 0.95 is required, the best operating conditions are—flow rate at 11–13 mL/min, sample concentration at 5.0–5.5 mg/mL, and mobile-phase composition at 80 hexane%. If a recovery yield higher than 0.90 is required, the best operating conditions are—flow rate at 11–13 mL/min, sample concentration at 6.5–7.0 mg/mL, and mobile-phase composition at 75 hexane%. However, for the *R*-isomer, the best operating conditions, which are not much different for the recovery yield higher than 0.90 or 0.95, are—flow rate at 10–12 mL/min, sample concentration at 5.0–5.5 mg/mL, and mobile-phase composition at 85 hexane%.

Finally, three selected optimum operating conditions and their corresponding system performance, once again verified by chromatographic experiments, are listed in Table 6. It can be seen that the agreement between the experimental results and the predicted system performance is reasonably

MARCEL DEKKER, INC.
270 Madison Avenue, New York, New York 10016

Table 4. Optimization Results for the *S*-Isomer

Weigh Factor (w)	Optimum Operating Conditions			System Performance	
	Flow Rate (mL/min)	Sample Concentration (mg/mL)	Mobile-Phase Composition (hexane%)	Production Rate (mg/min)	Specific Production (mg/mL)
(a) Recovery yield = 0.95					
0	20.98	5.23	80.19	3.897	0.186
0.05	13.07	5.48	80.61	3.541	0.271
0.10	11.33	5.68	80.97	3.304	0.292
0.15	10.31	5.86	81.29	3.121	0.303
0.20	9.55	6.03	81.59	2.964	0.310
0.25	8.90	6.20	81.92	2.815	0.316
0.30	8.27	6.40	82.29	2.661	0.322
0.35	7.53	6.68	82.82	2.470	0.328
0.40	5.91	7.31	84.07	2.036	0.344
(b) Recovery yield = 0.90					
0	19.20	6.30	74.82	4.861	0.253
0.05	13.46	6.51	75.08	4.462	0.331
0.10	11.78	6.71	75.32	4.179	0.355
0.15	10.83	6.87	75.53	3.969	0.366
0.20	10.15	7.02	75.72	3.796	0.374
0.25	9.60	7.16	75.90	3.642	0.379
0.30	9.12	7.30	76.09	3.499	0.384
0.35	8.66	7.45	76.29	3.357	0.388
0.40	8.19	7.62	76.53	3.203	0.391

MARCEL DEKKER, INC.
270 Madison Avenue, New York, New York 10016

Table 5. Optimization Results for the *R*-Isomer

Weigh Factor (w)	Optimum Operating Conditions			System Performance	
	Flow Rate (mL/min)	Sample Concentration (mg/mL)	Mobile-Phase Composition (hexane%)	Production Rate (mg/min)	Specific Production (mg/mL)
(a) Recovery yield = 0.95					
0	22.94	4.84	85.43	2.722	0.119
0.05	12.03	5.14	86.04	2.450	0.204
0.10	10.13	5.39	86.58	2.263	0.223
0.15	8.92	5.65	87.13	2.104	0.236
0.20	8.09	5.75	87.35	1.977	0.244
0.25	7.47	5.75	87.35	1.871	0.251
0.30	6.90	5.75	87.35	1.765	0.256
0.35	6.30	5.75	87.35	1.647	0.262
0.40	5.46	5.75	87.35	1.473	0.270
(b) Recovery yield = 0.90					
0	22.48	4.87	84.25	2.793	0.124
0.05	12.30	5.16	84.82	2.518	0.205
0.10	10.44	5.40	85.31	2.333	0.223
0.15	9.28	5.63	85.80	2.179	0.235
0.20	8.33	5.88	86.34	2.031	0.244
0.25	7.54	6.05	86.71	1.895	0.251
0.30	6.98	6.05	86.71	1.790	0.257
0.35	6.40	6.05	86.71	1.676	0.262
0.40	5.64	6.05	86.71	1.518	0.269

MARCEL DEKKER, INC.
270 Madison Avenue, New York, New York 10016

Table 6. Experimental Verification of the Three Selected Optimum Operating Conditions

(a) Optimum operating conditions

Run No.	Flow Rate (mL/min)	Sample Concentration (mg/mL)	Mobile-Phase Composition (hexane%)
1	13	5.66	80
2	14	6.60	75
3	12	5.05	85

(b) Corresponding system performance

Run No.	Type of Isomer for Collection	Purity (%)	Cycle Time (min)	Amount Collected (mg)	Recovery Yield (%)	Production Rate (mg/min)	Specific Production (mg/mL)
1	*S*-isomer	98	1.42	5.35	94.5	3.78	0.29
2	*S*-isomer	98	1.29	5.90	89.4	4.56	0.33
3	*S*-isomer	98	1.82	4.92	97.5	2.71	0.23

MARCEL DEKKER, INC.
270 Madison Avenue, New York, New York 10016

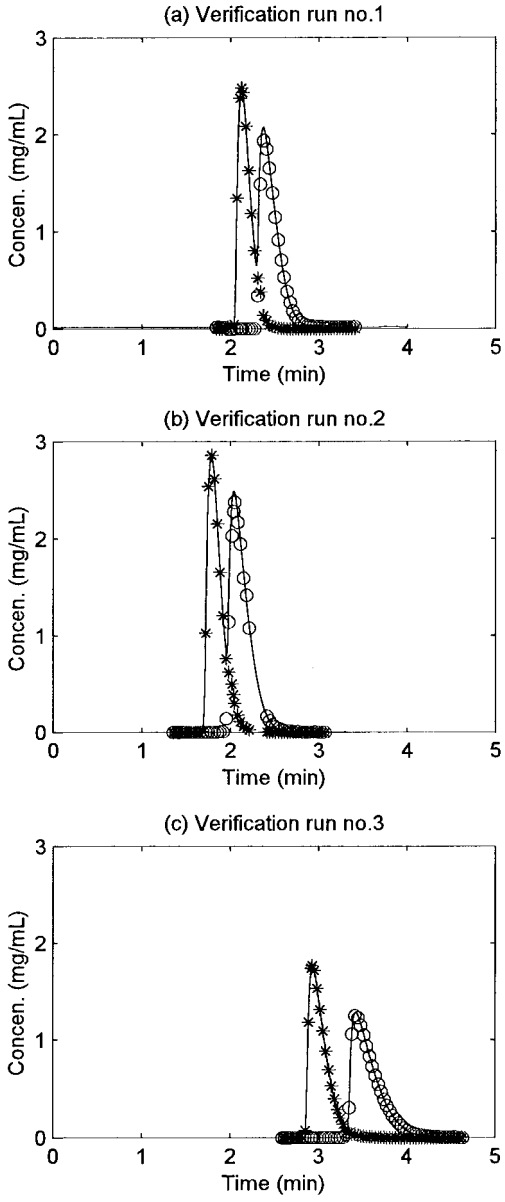

Figure 9. Experimental chromatograms of the three selected optimum conditions. (—): mixed band profile, (∗): band profile of the *S*-isomer and (○): band profile of the *R*-isomer.

MARCEL DEKKER, INC.
270 Madison Avenue, New York, New York 10016

good. By referring to their chromatograms, as shown in Fig. 9, the great effects of mobile-phase composition on the system performance for each isomer can be explained clearly by the degree of band overlapping. For the *S*-isomer collection, certain high degrees of band overlapping (Fig. 9a and b), and low level of hexane% in the mobile phase ($<80\%$) are allowed. However, only low degrees of band overlapping (Fig. 9c) and high level of hexane% in the mobile phase ($>85\%$) are allowed for the *R*-isomer collection.

CONCLUSIONS

Factorial design experiments using a spherical central composite design were applied to analyze the preparative separation of enantiomers of 1-1′-bi-2-naphthol on Pirkle covalent D-phenylglycine columns using hexane/isopropanol as the mobile phase. This study investigated the effect of three variables (flow rate, sample size, and mobile-phase composition) on the response functions (the production rate with or without solvent consumption) and established the regression models of second-order polynomials. Statistical analysis showed a good fit for each regression model.

The response surface analysis showed that in order to optimize both the production rate and the specific production (solvent consumption), the three operating variables are all significant and can be selected as follows. Hexane% in the mobile phase can be low ($<80\%$) for the *S*-isomer collection, but should be high ($>85\%$) for the *R*-isomer collection. No matter which isomer is desired, sample concentration can be as high as possible under its solubility limit and the requirement of the recovery yield; however, flow rate should be optimized on the basis of a compromise between the high production rate and the low solvent consumption.

The importance of the production rate and the solvent consumption was considered by the hybrid objective function, defined by Eq. (5). For the *S*-isomer collection, the optimum operating conditions are—flow rate at 11–13 mL/min, sample concentration at 5.0–5.5 mg/mL for the recovery yield higher than 0.95 or at 6.5–7.0 mg/mL for the recovery yield higher than 0.90, and mobile-phase composition at 80 hexane% for the recovery yield higher than 0.95 or at 75 hexane% for the recovery yield higher than 0.90. For the *R*-isomer collection, the best operating conditions, which are about the same for the recovery yield higher than 0.90 or 0.95, are—flow rate at 10–12 mL/min, sample concentration at 5.0–5.5 mg/mL, and mobile-phase composition at 85 hexane%. Finally, the separation results from the three selected optimum chromatographic experiments showed a good agreement with the predicted system performance.

MARCEL DEKKER, INC.
270 Madison Avenue, New York, New York 10016

NOMENCLATURE

C_i	solute concentration (mg/mL)
C_i^0	inlet concentrations of isomer i (mg/mL)
Pr_i	production rate of species i (mg/min)
Pr_i^*	a hybrid objective function defined by Eq. (5)
Q_f	solvent flow rate (mL/min)
SP_i	specific production (mg/mL)
$t_{ci,1}$	the beginning time of the collection of component i (min)
$t_{ci,2}$	the end time of the collection of component i (min)
V_in	sample volume (mL)
w	weight factor defined in Eq. (5) for the calculation of Pr_i^*
x_i	the coded levels of variable i
X_i	the actual levels of variable i
Y_i	recovery yield of a component i

Greek Letters

Δt_c	cycle time which separates two consecutive injections (min)

Subscripts

R	R-isomer
S	S-isomer

ACKNOWLEDGMENTS

The authors wish to thank the National Science Council of the Republic of China for the financial support under grant no. NSC 87-2214-E-224-005.

REFERENCES

1. Cohn, H. Large-Scale High-Performance Preparative Liquid Chromatography. In *Preparative and Process-Scale Liquid Chromatography*; Subramanian, G. Ed.; Ellis Horwood: New York, 1991.
2. Krakel, J. N.; Cabrera, K.; Eisenbeiss, F. Preparative Direct Chromatographic Separation of Enantiomers on Chiral Stationary Phases. In *Preparative and Production Scale Chromatography*; Ganetsos, G., Barker, P. E. Eds.; Marcel Dekker: New York, 1993.
3. Katti, A.M.; Guiochon, G. Quantitative Comparison Between the Experimental Band Profiles of Binary Mixtures in Overloaded Elution Chromatography and Their Profiles Predicted by the Semi-Ideal Model. J. Chromatogr. **1990**, *499*, 21–35.

4. Jacobson, S.; Golshan-Shirazi, S.; Guiochon, G. Chromatographic Band Profiles and Band Separation of Enantiomers at High Concentration. J. Am. Chem. Soc. **1990**, *112*, 6492–6498.
5. Jacobson, S.; Golshan-Shirazi, S.; Guiochon, G. Isotherm Selection for Band Profile Simulations in Preparative Chromatography. AIChE J. **1991**, *37* (6), 836–844.
6. Lai, S.-M.; Lin, Z.-C.; Loh, R.-R. Optimization of the Separation of 1-1′-Bi-2-naphthol Enantiomers in Preparative Liquid Chromatography. J. Chin. Inst. Chem. Eng. **2000**, *31* (5), 507–522.
7. Montgomery, D.C. *Design and Analysis of Experiments*; 4th Ed.; John Wiley and Sons: New York, 1997; Chap. 14.
8. Rosini, C.; Franzini, L.; Raffaelli, A.; Salvadori, P. Synthesis and Applications of Binaphthylic C_2-Symmetry Derivatives as Chiral Auxiliaries in Enantioselective Reactions. Synthesis **1992**, *503*, 503–517.
9. Hattori, K.; Yamamoto, H. Asymmetric Aza-Diels–Alder Reaction: Enantio- and Diastereoselective Reaction of Imine Mediated by Chiral Lewis Acid. Tetrahedron **1993**, *49* (9), 1749–1760.
10. Myers, R.H.; Montgomery, D.C. *Response Surface Methodology: Process and Product Optimization Using Designed Experiments*; John Wiley and Sons: New York, 1995; Chaps. 6 & 7.
11. Felinger, A.; Guiochon, G. Optimizing Experimental Conditions for Minimum Production Cost in Preparative Chromatography. AIChE J. **1994**, *40* (4), 594–605.
12. Schittowski, K. A FORTRAN-Subroutine Solving Constrained Nonlinear Programming Problems. Ann. Oper. Res. **1985**, *5*, 485–500.

Received February 2001

MARCEL DEKKER, INC.
270 Madison Avenue, New York, New York 10016

Request Permission or Order Reprints Instantly!